

energies. Consideration will be given to autoionization following double-electron-capture events. The relative importance of the single-capture, transfer-ionization, and autoionization n distributions will be examined. Atomic units will be used throughout.

II. THEORY

In this work, we will mainly be interested in studying the capture cross section, $\sigma_{q,q-1}$, which is obtained by summing the cross sections for reactions (1a), (1b), and (1d). In addition to the procedures used in our previous CTMC calculations,^{1,2} the final (n,l) sublevels of the product state of the captured electrons has to be determined, including the possibility of autoionization.

To make a correspondence between classical binding states and quantum (n,l) levels, we use the quantization rules derived by Becker and MacKellar.²⁵ Classical quantum numbers denoted by n_c and l_c are defined in terms of the binding energy U and the Cartesian coordinates (x,y,z) of the captured electron with regard to the projectile nucleus as follows:

$$n_c = q / (-2U)^{1/2}, \quad (2)$$

$$l_c = [(x\dot{y} - y\dot{x})^2 + (x\dot{z} - z\dot{x})^2 + (y\dot{z} - z\dot{y})^2]^{1/2}. \quad (3)$$

The quantum numbers n and l are then obtained by

$$[(n-1)(n-\frac{1}{2})n]^{1/3} \leq n_c \leq [n(n+\frac{1}{2})(n+1)]^{1/3}, \quad (4)$$

$$l \leq \frac{n}{n_c} l_c \leq l+1. \quad (5)$$

Tens of thousands of trajectories for n distributions and more for the (n,l) distributions are usually needed to keep statistical uncertainties within 10%.

For multiply charged ions impinging on H_2 or He , double capture could result in autoionization of one electron to the continuum and decay of the other electron to a lower n state. Therefore, a certain fraction of the double-capture cross section has to be added to the transfer-ionization cross section.¹

In an effort to take the autoionization process into account, Hamilton's equations of motion for each of the two independent target electrons are solved simultaneously for a given set of initial conditions. In the event that two electrons are captured, we monitor the final one-electron binding energies (U_1 and U_2) referred to the projectile. If both electrons are captured to one-electron excited states, i.e., U_1 and U_2 are outside the ground-state bin $(-\infty, -q^2/(2 \times 3^{2/3}))$ obtained from Eq. (4), we assume that one electron will be ionized whereas the other one will remain bound to the projectile with a binding energy $U = U_1 + U_2$. Thus, we assume 100% branching to the Auger process rather than to radiative decay. If one of the two electrons is captured to the ground state of the projectile, i.e., U_1 or U_2 is smaller than $-q^2/(2 \times 3^{2/3})$, then no autoionization can occur.

Since the CTMC method does not predict possible changes of the angular momenta of the doubly captured electrons during the autoionization process, the l dependence has not been studied for electron capture by multi-

ply charged ions with $q \geq 2$, except when the double-capture channel is negligible. Thus, it is possible to investigate the proton impact case and multiply-charged-ion systems when the electron is captured to a sufficiently high n level for which the contribution of the autoionization channel is negligible.

III. RESULTS

As a benchmark of our model for molecular hydrogen, we compare in Fig. 1 the theoretical capture cross sections into different (n,l) states for $H^+ + H_2$ collisions with various experimental data. As can be clearly seen in this figure, our CTMC calculations predict, in general, both the shape and magnitude of the experimental (n,l) distributions. Specifically, the theoretical results agree well with the experimental data for the 2s, 3s, and 2p states, but lie somewhat above the data for the 4s state. For the 3p state, our calculations lie between two different sets of data that disagree with each other.

Similarly, a benchmark of our model for helium is made in Fig. 2, where we display the CTMC cross sections for electron capture into different (n,l) states in $H^+ + He$ collisions which are compared with various experimental data and the coupled-channel calculation of Jain *et al.*²³ using an atomic-base expansion. Similar conclusions to those obtained for H_2 are reached in this

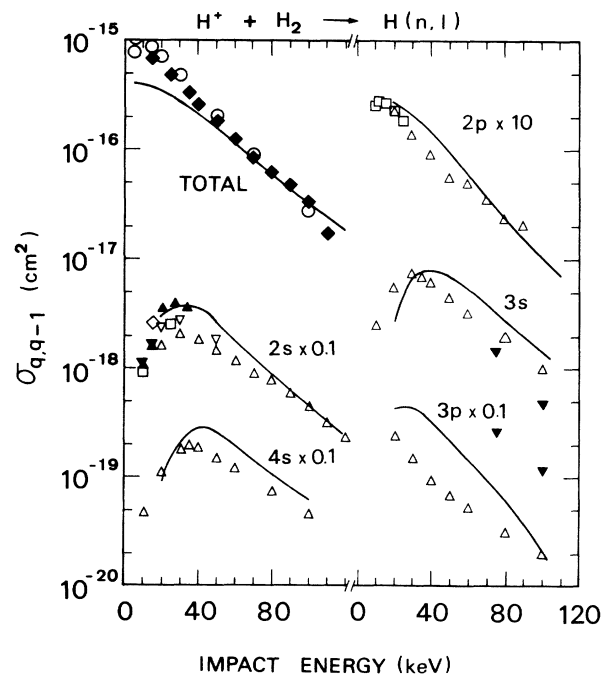


FIG. 1. The (n,l) distributions of $\sigma_{q,q-1}$ in $H^+ + H_2 \rightarrow H(n,l)$ collisions. Solid curves, present work; \circ , Rudd *et al.* (Ref. 3); \blacklozenge , De Heer *et al.* (Ref. 4); \triangle , Hughes *et al.* (Refs. 5–8); \diamond , Shah *et al.* (Ref. 9); \square , Birely and McNeal (Ref. 10); \blacktriangle , Andreev *et al.* (Ref. 11); ∇ , Bayfield (Ref. 12); \blacktriangledown , Ford and Thomas (Ref. 13).

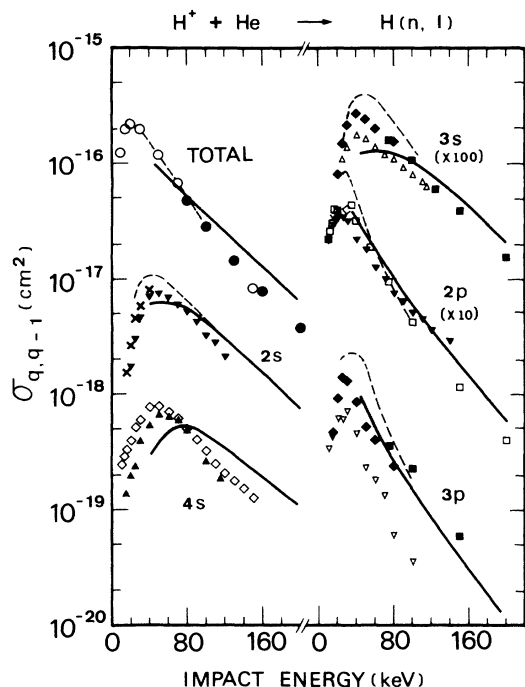


FIG. 2. The (n, l) distributions of $\sigma_{q, q-1}$ in $H^+ + He \rightarrow H(n, l)$ collisions. Solid curves, present work. At impact energies smaller than 80 keV the statistical uncertainties of the capture cross sections to the 4s, 3s, and 3p states are 20%. Dashed curves, coupled-channel calculations by Jain *et al.* (Ref. 23); \triangle , \blacktriangle , ∇ , \blacktriangledown , Hughes *et al.* (Refs. 5–7 and 14); \blacksquare , Ford and Thomas (Ref. 13); \square , Hippler *et al.* (Refs. 15 and 16); \diamond , Doughty *et al.* (Ref. 17); \times , Andreev *et al.* (Ref. 11); \blacklozenge , Lenormand (Ref. 18); \bullet , Shah and Gilbody (Ref. 19); \circ , Rudd *et al.* (Ref. 3).

case, except for capture to the 4s state where the CTMC method does not predict the position of the experimental maximum.

In Fig. 3 we compare the theoretical and experimental total capture cross sections, $\sigma_{q, q-1}$, in collisions of multiply charged ions with atomic helium. Two CTMC calculations are displayed in the figure, which consist of representing the electron–target-core ($e^- - He^+$) interaction by means of either an effective Coulomb potential or a model potential.² In the expected validity range ($E \gtrsim 50$ keV/amu), the results obtained with the effective Coulomb potential are in excellent agreement with the experimental data for proton impact. However, the model potential produces cross sections in better agreement with experiment for other charge states in the higher-energy range displayed in the figure. The reason for the discrepancies observed for a model potential for proton impact is that the binding energies of captured electrons adopt unphysical values below the ground state of hydrogen. This is a well-known problem in CTMC calculations that is usually observed when the initial binding energy is greater than the ground-state energy of the projectile. In the present case, this problem is expected to cause trouble when describing the electron capture to the ground state

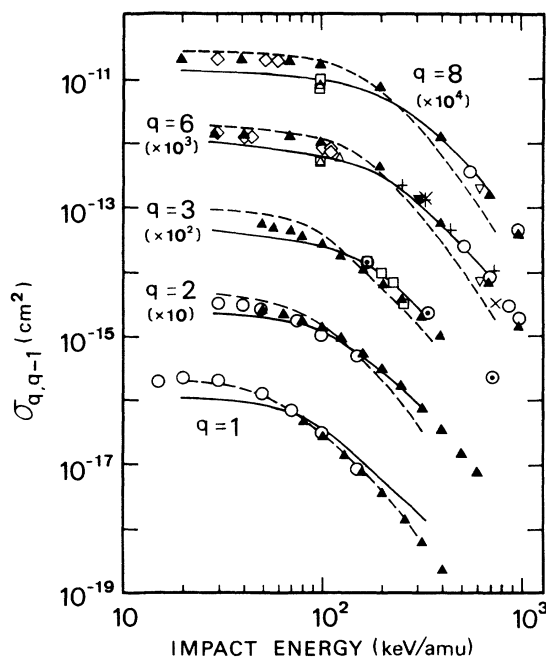


FIG. 3. Total capture cross sections, $\sigma_{q, q-1}$, in collisions of multiply charged ions with atomic helium. Solid curves, present CTMC calculations with a model potential; dashed curves, CTMC calculations with an effective Coulomb potential. Experimental data for H^+ , He^{2+} , and Li^{3+} : \circ , Rudd *et al.* (Ref. 26); \blacktriangle , Shah and Gilbody (Ref. 19); \square , Pivovar *et al.* (Ref. 27); \odot , Nicolaev *et al.* (Ref. 28). C^{6+} and O^{8+} : \blacktriangle , Janev *et al.* (Ref. 29); \diamond , Bayfield *et al.* (Ref. 30); \triangle , Knudsen *et al.* (Ref. 31); $+$, Nikolaev *et al.* (Ref. 28); \circ , Dillingham *et al.* (Ref. 32); \square , Datz *et al.* (Ref. 33); \blacktriangledown , Graham *et al.* (Ref. 34); ∇ , MacDonald and Martin (Ref. 35); \times , Dmitriev *et al.* (Ref. 36).

of hydrogen but not for higher n levels.

In Figs. 4 and 5 we display the n distribution for $\sigma_{q, q-1}$ in collisions of He with ions of charge 1 to 10 at 50 and 100 keV/amu, respectively. In these calculations and the following, we have utilized the model potential to account for the interaction between the target electrons. Also shown in these figures are the experimental data for proton impact obtained from the measured (n, l) distributions of Fig. 1, as well as the spectroscopic data of Refs. 21 and 22 for O^{6+} projectiles. Our calculations are in very good agreement with the data for proton impact, whereas discrepancies between a factor of 1.5 and 2.5 can be seen in Fig. 5 for O^{6+} impact, our cross section for C^{6+} projectiles being too small.

As can be seen in Figs. 4 and 5, the capture cross sections for H^+ and He^{2+} impact present their maximum at the ground level, whereas the maxima of the capture cross sections for $q > 2$ are at excited levels. In general, the maximum shifts to higher electronic levels for increasing projectile charges. For a fixed charge, the maxima remain at almost the same place for the two energies considered, but broaden with increasing energy. For high projectile charges it is seen that the maximum splits into two different maxima. Separation of $\sigma_{q, q-1}$ into the

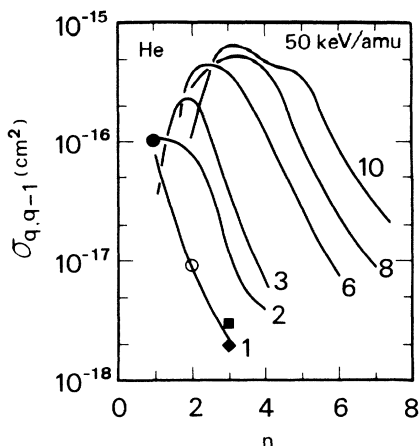


FIG. 4. The n distribution of $\sigma_{q,q-1}$ in $A^{q+} + \text{He}$ collisions at 50 keV/amu. The numbers in the figure indicate the projectile charges. Solid curves, present work. Experimental data for H^+ on He: ●, Refs. 3, 5, and 18; ○, Hughes *et al.* (Ref. 5); ◆, Hughes *et al.* (Refs. 6 and 14); ■, Lenormand (Ref. 18).

different capture channels indicates that while the first peak is due to the autoionization channel, the second peak at large n values comes mainly from the single-capture channel.

In previous works for atomic hydrogen targets,^{37,38} the position of the maxima could be explained in terms of a simple picture that assumes conservation of the binding energy and the dimensions of the orbit during the electron-capture process. As a consequence of these considerations, the product n distribution was found to maximize at

$$n_{\max} = \frac{1}{(2I_i)^{1/2}} q^{3/4}, \quad (6)$$

where I_i is the ionization potential of the target (i.e.,

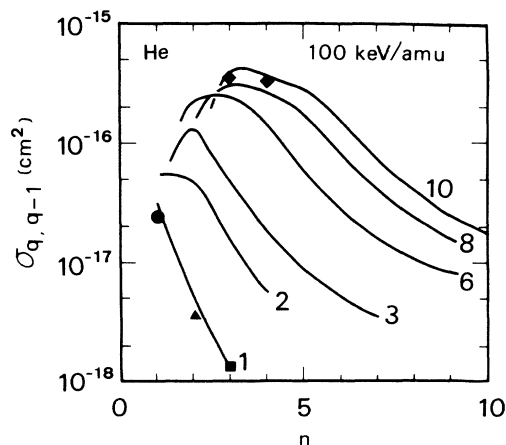


FIG. 5. The n distribution of $\sigma_{q,q-1}$ in $A^{q+} + \text{He}$ collisions at 100 keV/amu. The numbers in the figure indicate the projectile charges. Experimental data for H^+ on He: ●, Refs. 3, 5, and 18; ■, Ford and Thomas (Ref. 13); ▲, Hughes, *et al.* (Ref. 5). O^{6+} on He: ◆, Dunford and Liu, *et al.* (Refs. 21 and 22).

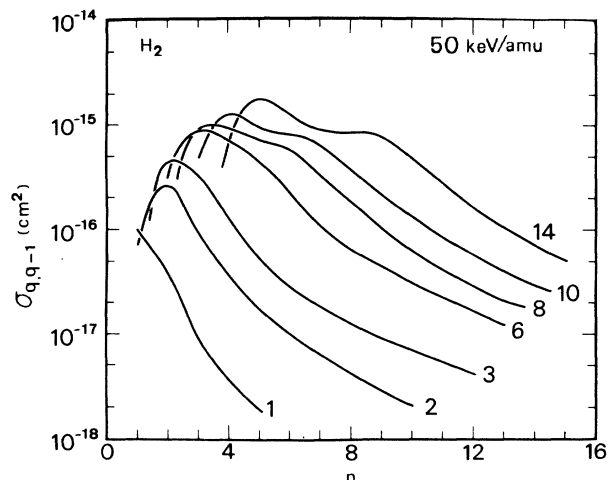


FIG. 6. Present CTMC calculations of the n distribution of $\sigma_{q,q-1}$ in $A^{q+} + \text{H}_2$ collisions at 50 keV/amu. The numbers in the figure indicate projectile charges.

$I_i = 0.5, 0.567,$ or 0.904 a.u. for H, H_2 , or He, respectively).

For helium targets, we have observed a similar pattern to Eq. (6) for the single-capture cross sections, reaction (1a), but not for $\sigma_{q,q-1}$. This is easily understood since the autoionization subset of $\sigma_{q,q-1}$ does not obey Eq. (6).

Figure 6 shows the n distribution of the cross section for electron capture from H_2 by ions of charge 1–14 at 50 keV/amu. Likewise the results at 100 keV/amu are shown in Fig. 7. These distributions have a similar shape to those obtained for He, but are spread over a wider range of n levels. This can be explained in terms of the differences in the relative velocities v_p/v_e for H_2 and He, where v_e is the initial orbital velocity of the electron and v_p is the impact velocity of the projectile.

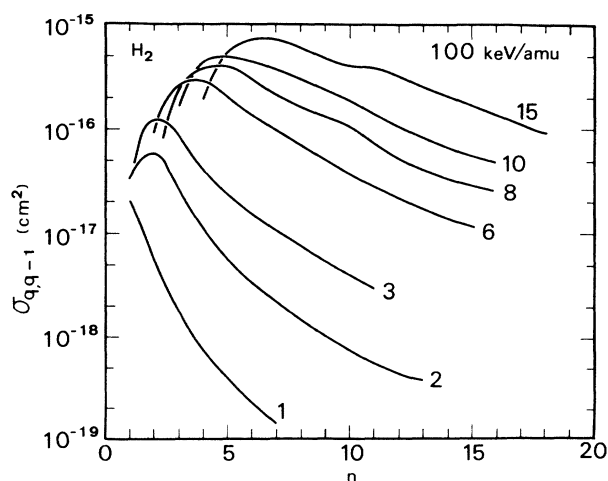


FIG. 7. Present CTMC calculations of the n distribution of $\sigma_{q,q-1}$ in $A^{q+} + \text{H}_2$ collisions at 100 keV/amu. The numbers in the figure indicate the projectile charges.

Similar conclusions as for He are also obtained for the maxima of the single-capture cross sections. In this case, we have found that the position of the maxima of the single-capture cross sections follow approximately the scaling $n_{\max} = 1.3q^{3/4}$. On the other hand, the maxima of $\sigma_{q,q-1}$ at the two impact energies displayed in the figures are close to each other and their positions can be found at approximately $n_{\max} = 1.1q^{0.6}$.

In order to show the relative magnitudes of the competing electron-capture channels, the n distribution for the case of $A^{14+} + H_2$ collisions at 100 keV/amu is separated in Fig. 8 into its single-capture, direct transfer-ionization, and autoionizing double-capture components. In this case, direct transfer-ionization is small in comparison with the n distribution of $\sigma_{q,q-1}$. On the other hand, autoionizing double capture provides a significant contribution to the capture cross section, which prevails to low-lying n levels. For $n > 10$, autoionization becomes negligible and single capture dominates and follows the well-known n^{-3} scaling for large values of n . Thus, inclusion of autoionization in $\sigma_{q,q-1}$ results in a shift of the maximum towards low-lying levels.

In Fig. 8 we also display the experimental data of Sørensen *et al.*,²⁰ which were obtained in $Au^{14+} + H_2$ collisions. As we will show below, the major contribution to the n distribution for $n \geq 10$ comes from large values of l that correspond to quasicircular orbits. Therefore, core effects (i.e., effects due to the electrons in the partially stripped Au^{14+} core) are not expected to be appreciable for the measured n distributions. Surprisingly, a clear disagreement is observed between the theoretical calculations and the experimental data as to both the magnitude and the shape of the cross sections. This disagreement cannot be explained in terms of a systematic difference in the normalization of the cross sections since the experimental and theoretical total cross sections to all n levels differ by a factor of 1.8, whereas the departures in the n distributions are as much as a factor between 2.8 and 4.3. On the other hand, if we neglect autoionization in our

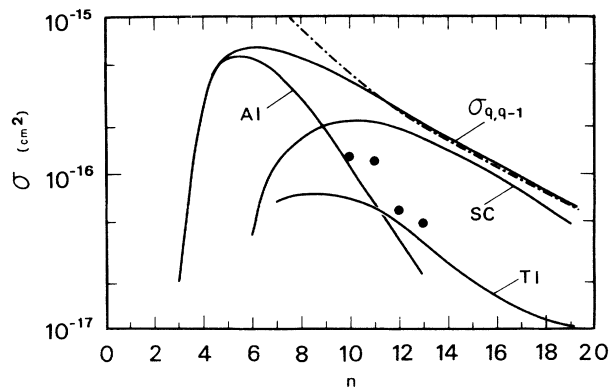


FIG. 8. The n distribution of the total capture cross section $\sigma_{q,q-1}$ for $A^{14+} + H_2$ collisions at 100 keV/amu is separated into its components: single capture (SC), transfer ionization (TI), and autoionization (AI) following double-capture events. Solid curves, present work; Dash-dotted curve, n^{-3} scaling; solid circles, Sørensen *et al.* (Ref. 20) for $Au^{14+} + H_2$.

calculations due to possible core effects, the CTMC cross section for single capture plus transfer ionization to all n levels is $2.96 \times 10^{-15} \text{ cm}^2$, which is in very good agreement with the experimental value of $3.02 \times 10^{-15} \text{ cm}^2$ for $\sigma_{q,q-1}$. However, large differences still persist between the measured n distribution and the calculated n distribution for the single-capture channel alone.

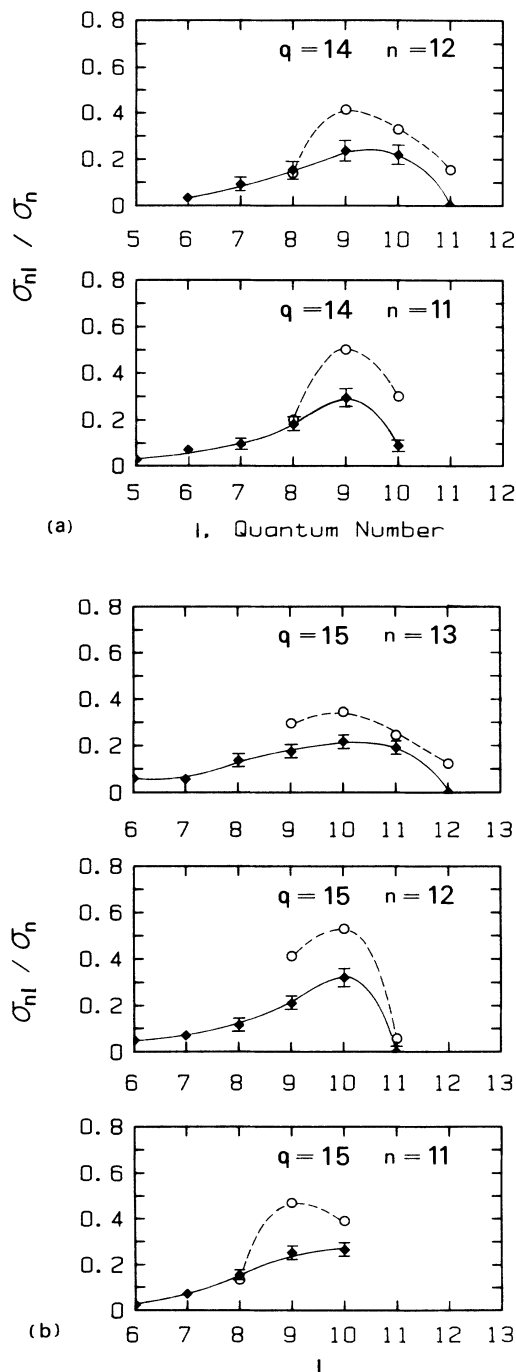


FIG. 9. The ratios between the cross section for electron capture to an n and l level and that to the n level in collisions of H_2 with projectiles of (a) $q = +14$ and (b) $q = +15$. Solid curves with error bars, present work; dashed curves and open circles, Sørensen *et al.* (Ref. 20).

On the basis of the calculations presented in Fig. 8, we conclude that, for $A^{14+} + \text{H}_2$ collisions at 100 keV/amu, autoionization is negligible in comparison with single capture and transfer ionization when $n \geq 10$. Therefore, the l distribution of the captured electrons can be defined for these n levels in terms of single capture and transfer ionization. Figure 9 shows the ratios between the cross sections for capture to an (n, l) level and those to the n level. In this case, the n_{max} for single capture are found to be 9 and 10 for $q = 14$ and 15. The n states considered here are thus above n_{max} . For these n values, both theoretical and experimental l distributions show a maximum at $l_{\text{max}} \approx n_{\text{max}}$, which is independent of the n values considered.

The transfer of the electron to this preferred l value can be explained in a simple picture as has been done before for atomic hydrogen targets.³⁷ Our calculations show that the most probable contribution to the total capture cross section comes from impact parameters of about 5.2 a.u. for both $q = 14$ and 15. Thus, electrons captured by a projectile of 100 keV/amu ($v_p = 2.0$ a.u.) at

this impact parameter would have a most probable angular momentum of $l \approx 10$.

IV. SUMMARY

We have applied the CTMC method to the study of the total capture cross sections for $A^{q+} + \text{He}$ collisions as well as the subshell electron-capture cross sections in collisions of multiply charged ions with H_2 and He. In general, good agreement with experimental data has been found. The possibility of autoionization after double capture has been modeled and this reaction channel has been found to influence the shape of the n distributions for low-lying n levels. In situations for which the autoionizing double-capture is negligible, electrons are found to be captured to a preferred l state ($l_{\text{max}} \approx n_{\text{max}}$), which is independent of n when $n > n_{\text{max}}$.

ACKNOWLEDGMENTS

We would like to thank the Office of Fusion Research of the U.S. Department of Energy for its support.

- ¹L. Meng, C. O. Reinhold, and R. E. Olson, Phys. Rev. A **40**, 3637 (1989).
- ²C. O. Reinhold and C. A. Falcon, Phys. Rev. A **33**, 3859 (1986).
- ³M. E. Rudd, R. D. DuBois, L. H. Toburen, C. A. Ratcliffe, and T. V. Goffe, Phys. Rev. A **28**, 3244 (1983).
- ⁴F. J. de Heer, J. Schutten, and H. Moustafa, Physica **32**, 1766 (1966).
- ⁵R. H. Hughes, E. D. Stokes, Song-Sik Choe, and T. J. King, Phys. Rev. A **4**, 1453 (1971).
- ⁶R. H. Hughes, C. A. Stigers, B. M. Doughty, and E. D. Stokes, Phys. Rev. A **1**, 1424 (1970).
- ⁷R. H. Hughes, H. R. Dawson, and B. M. Doughty, Phys. Rev. **164**, 166 (1967).
- ⁸R. H. Hughes, T. J. King, and Song-Sik Choe, Phys. Rev. A **5**, 644 (1972).
- ⁹M. B. Shah, J. Geddes, and H. B. Gilbody, J. Phys. B **15**, 4049 (1980).
- ¹⁰J. H. Birely and R. J. McNeal, Phys. Rev. A **5**, 692 (1972).
- ¹¹E. P. Andreev, V. A. Ankudinov, and S. V. Bobashev, in *Abstracts of Papers of the Fifth International Conference on the Physics of Electronic and Atomic Collisions, Leningrad, 1967*, edited by I. P. Flaks *et al.* (Nauka, Leningrad, 1967), p. 309.
- ¹²J. E. Bayfield, Phys. Rev. **182**, 115 (1969).
- ¹³J. C. Ford and E. W. Thomas, Phys. Rev. A **5**, 1694 (1972).
- ¹⁴R. H. Hughes, H. R. Dawson, B. M. Doughty, D. B. Kay, and C. A. Stigers, Phys. Rev. **146**, 53 (1966).
- ¹⁵R. Hippler, W. Harbich, M. Faust, H. O. Lutz, and L. J. Dube, J. Phys. B **19**, 1507 (1986).
- ¹⁶R. Hippler, W. Harbich, H. Madeheim, H. Kleinpoppen, and H. O. Lutz, Phys. Rev. A **35**, 3139 (1987).
- ¹⁷B. M. Doughty, M. L. Goad, and R. W. Cernosek, Phys. Rev. A **18**, 29 (1978).
- ¹⁸J. Lenormand, J. Phys. **37**, 699 (1976).
- ¹⁹M. B. Shah and H. B. Gilbody, J. Phys. B **18**, 899 (1985).
- ²⁰J. Sørensen, L. H. Andersen, P. Hvelplund, H. Knudsen, L. Liljeby, and E. H. Nielsen, J. Phys. B **17**, 4743 (1984).
- ²¹R. W. Dunford, C. J. Liu, H. G. Berry, R. C. Pardo, and M. L. A. Raphaelian, Phys. (Paris) Colloq. **50**, C1-337 (1989).
- ²²C. J. Liu, R. W. Dunford, H. G. Berry, R. C. Pardo, K. O. Groeneveld, M. Hass, and M. L. A. Raphaelian, J. Phys. B **22**, 1217 (1989).
- ²³Ashok Jain, C. D. Lin, and W. Fritsch, Phys. Rev. A **36**, 2041, (1987).
- ²⁴W. Fritsch and C. D. Lin, J. Phys. B **19**, 2683 (1986).
- ²⁵R. L. Becker and A. D. MacKellar, J. Phys. B **17**, 3923 (1984).
- ²⁶M. E. Rudd, T. V. Goffe, and A. Itoh, Phys. Rev. A **32**, 2128 (1985).
- ²⁷L. I. Pivovarov, Yu. Z. Levchenko, and G. A. Krivonosov, Zh. Eksp. Teor. Fiz. **39**, 19 (1970) [Sov. Phys.—JETP **32**, 11 (1971)].
- ²⁸V. S. Nikolaev, I. S. Dmitriev, L. N. Fateeva, and Ya. A. Teplova, Zh. Eksp. Teor. Fiz. **40**, 989 (1961) [Sov. Phys.—JETP **13**, 695 (1961)].
- ²⁹R. K. Janev, R. A. Phaneuf, and H. T. Hunter, At. Data. Nucl. Data Tables **40**, 249 (1980).
- ³⁰J. E. Bayfield, L. D. Gardner, Y. Z. Gulkok, T. K. Saylor, and S. D. Sharma, Rev. Sci. Instrum. **51**, 651 (1980).
- ³¹H. Knudsen, H. K. Haugen, and P. Hvelplund, Phys. Rev. A **23**, 597 (1981).
- ³²T. R. Dillingham, J. R. MacDonald, and P. Richard, Phys. Rev. A **24**, 1237 (1981).
- ³³S. Datz, R. Hippler, L. H. Andersen, P. F. Dittner, H. Knudsen, H. F. Krause, P. D. Miller, P. L. Pepmiller, T. Rosseel, N. Stolterfoht, Y. Yamazaki, and C. R. Vane, Nucl. Instrum. Methods Phys. Res. A **262**, 62 (1987).
- ³⁴W. G. Graham, K. H. Berkner, R. V. Pyle, A. S. Schlachter, J. W. Stearns, and J. A. Tanis, Phys. Rev. A **30**, 722 (1984).
- ³⁵J. R. MacDonald and F. W. Martin, Phys. Rev. A **4**, 1965 (1971).
- ³⁶I. S. Dmitriev, V. S. Nikolaev, Yu. A. Tashaev, and Ya. A. Teplova, Zh. Eksp. Teor. Fiz. **67**, 2047 (1974) [Sov. Phys.—JETP **40**, 1017 (1975)].
- ³⁷R. E. Olson, Phys. Rev. A **24**, 1726 (1981).
- ³⁸R. E. Olson and D. R. Schultz, Phys. Scr. **T28**, 71 (1989).